ELECTRON-PROTON INSTABILITIES FOR INTENSE PROTON RINGS

K. Y. Ng

Fermi National Accelerator Laboratory, P.O. Box 500, Batavia, IL 60510*

Abstract

Electron-proton instabilities are compared among the high-intensity Fermilab future booster, the Oak Ridge SNS storage ring, the Los Alamos PSR, and the Brookhaven booster. All these 4 machines have proton intensities ranging from 2.4×10^{13} to 1×10^{14}. The escape rates of single electrons from the bunch gaps are computed. The threshold neutralization factors for coherent centroid-oscillation for proton and electron beams are derived. The energies of electron escaping from the bunch hitting the walls of the beam pipe are estimated so as to determine whether multipactoring will occur or not. Finally, the reasons why e-p instabilities have not been observed at the Rutherford ISIS are discussed.

Submitted to the 8th Advanced Beam Dynamics Mini-Workshop on Two-Stream Instabilities in Particle Accelerators and Storage Rings
Santa Fe, New Mexico
February 16-18, 2000

*Operated by the Universities Research Association, Inc., under contract with the U.S. Department of Energy.

I INTRODUCTION

There is an investigation underway at Fermilab for the design of a high-intensity booster to serve as the proton driver for a neutrino factory or muon collider [1]. The total number of particles stored will be at least 3.36×10^{13}, to be upgraded to more than 1×10^{14} in the future. The PSR at Los Alamos (LANL) running with 2.3 to 4.2×10^{13} protons has always been troubled by the electrons trapped inside the proton beam [2]. Recently, it has also been reported that the Brookhaven (BNL) booster running in the coasting-beam mode with 3.7×10^{13} protons experiences sudden fast beam loss which appears to be the result of e-p instabilities [3]. For this reason, it is an important task to examine whether e-p instabilities will play a detrimental role in the future Fermilab booster. Electron-proton instabilities will occur most possibly during multi-turn injection when the gaps between bunches are small. As the bunches are ramped, the bunches become much shorter inside the accelerating buckets leaving much large gaps for the trapped electrons to escape. As a result, we will investigate here only the situation during multi-turn injections. There is a spallation neutron source (SNS) with a storage ring of similar intensity under construction at Oak Ridge (ORNL) [4], and we will include it also in our comparison. The important data of the various rings are listed in Table I. For the LANL PSR, the designed intensity of the upgraded storage ring, 4.2×10^{13}, is used. For the BNL booster, the highest bunched beam intensity of 2.4×10^{13} is considered. The analysis will follow mostly Refs. [2, 5, 6, 7].

II SINGLE-ELECTRON MECHANICS

Electrons inside the vacuum chamber are supposed not to move longitudinally. As the proton bunch passes through them, they are attracted towards the central axis of the proton bunch with vertical electron *bounce frequency* $\Omega_e/(2\pi)$ given by [7]

$$\Omega_e^2 = \frac{4Nr_e c^2}{a'(a+a')L_b} \ . \tag{2.1}$$

Here, N_p is the number of protons in the bunch which has an elliptical cross section

Table I: Some data of the Fermilab future booster, the Oak Ridge SNS, the Los Alamos PSR, and the Brookhaven booster at injection.

	Fermilab Booster	Oak Ridge SNS	Los Alamos PSR	Brookhaven Booster
Circumference C (m)	711.3040	220.6880	90.2000	201.769
Injection kinetic energy (GeV)	0.400	1.000	0.797	0.200
γ	1.4263	2.0658	1.8494	1.2132
β	0.7131	0.8750	0.8412	0.5662
Revolution frequency f_0 (MHz)	0.3005	1.1887	2.7959	0.8412
Revolution period T_0 (ns)	3327	841.3	357.7	1189
Total number of protons N_p	3.36×10^{13}	10.0×10^{13}	4.2×10^{13}	2.4×10^{13}
Rf harmonic (no. of bunches) h	4	1	1	1
Number of injection turns	27	1225	2000	300
Repetition rate (Hz)	15	60	12	7.5

with vertical and horizontal radii a and a', L_b is the full bunch length, r_e the electron classical radius, and c the velocity of light. We assume that the proton beam has uniform longitudinal and radial distribution and has a cylindrical cross section with radius a inside a cylindrical beam pipe of radius b. Thus $a'(a+a')$ can be replaced by $2a^2$. The images of the proton beam and the electron cloud in the walls of the vacuum chamber will modify the electron bounce frequency depicted in Eq. (2.1), but their effects are neglected in this study. Also, only linear focusing force by the proton beam on the electrons is considered.

An electron trapped inside the proton beam performs betatron oscillations with an equivalent betatron function $\beta_b = \beta c/\Omega_e$ with a total betatron phase advance $\phi_b = \Omega_e L_b/v$, where βc is the velocity of the protons. After the passage of the proton bunch, the motion of the electron in the gap is equivalent to a drift of length $L_g = \lambda_{\rm rf} - L_b$ with $\lambda_{\rm rf}$ being the rf wavelength or stationary bucket width. Here, we

Table II: Instability and escape time through the bunch gap of a single electron trapped inside the proton bunches of the Fermilab booster, ORNL SNS, LANL PSR, and BNL booster.

	Fermilab Booster	Oak Ridge SNS	Los Alamos PSR	Brookhaven Booster
Injection full bunch length (m)	118.55	143.39	60.13	100.89
Gap length (m)	59.28	77.30	30.07	100.89
Proton beam radius a (m)	0.0235	0.0380	0.0150	0.0150
Bounce angular frequency Ω_e	255.1	713.3	1253.9	462.6
Bounce betatron phase ϕ_b (rad)	141.47	58.57	115.0	64.68
$\frac{1}{2}\lvert\mathrm{Tr}M\rvert$	2.53	94.91	70.79	132.7
Escape time in no. of rf buckets	0.6324	0.1906	0.2019	0.1792

assume all rf buckets are filled. The transfer matrix for an rf wavelength is [2]

$$M = \begin{pmatrix} 1 & L_g \\ 0 & 1 \end{pmatrix} \begin{pmatrix} \cos\phi_b & \beta_b \sin\phi_b \\ -\dfrac{1}{\beta_b}\sin\phi_b & \cos\phi_b \end{pmatrix} = \begin{pmatrix} \cos\phi_b - \dfrac{L_g}{\beta_b}\sin\phi_b & \beta_b \sin\phi_b + L_g \sin\phi_b \\ -\dfrac{1}{\beta_b}\sin\phi_b & \cos\phi_b \end{pmatrix} . \tag{2.2}$$

In order that the electron will not be trapped inside the proton bunch, its motion has to be unstable or

$$\frac{1}{2}|\mathrm{Tr}M| = \left|\cos\phi_b - \frac{L_g}{2\beta_b}\sin\phi_b\right| > 1 \ . \tag{2.3}$$

If the electron is unstable, we can write

$$\frac{1}{2}|\mathrm{Tr}M| = \cosh\mu \ , \tag{2.4}$$

where $\mu\beta c/\lambda_{\mathrm{rf}}$ is the growth rate of the electron oscillation amplitude, and μ^{-1} is the growth time in rf buckets. These are computed for all the 4 rings and the results are listed in Table II. We see that for all the 4 rings, the electrons trapped should be able to escape to the walls of the beam pipe in the beam gap.

Sometimes, the gap is not totally free of protons. The space-charge effect of the protons will distort the rf bucket reducing its momentum acceptance. As a result,

some protons may leak out of the bucket and end up in the bunch gap. If a fraction η of the proton leaks into the gap, the electron will oscillate with bounce frequency $\Omega_{eb}/(2\pi)$ inside the proton beam and bounce frequency $\Omega_{eg}/(2\pi)$ in the bunch gap. These frequencies are given by [2, 5]

$$\Omega_{eb}^2 = \Omega_e^2(1-\eta) \qquad \text{and} \qquad \Omega_{eg}^2 = \Omega_e^2\eta \ . \tag{2.5}$$

Again, only linear focusing force by the proton beam is considered. The betatron phase advances in the beam and in the gap are, respectively, $\phi_b = \Omega_{eb}L_b/(\beta c)$ and $\phi_g = \Omega_{eb}L_g/(\beta c)$. The transfer matrix is therefore

$$M = \begin{pmatrix} \cos\phi_g & \beta_g \sin\phi_g \\ -\dfrac{1}{\beta_g}\sin\phi_g & \cos\phi_g \end{pmatrix} \begin{pmatrix} \cos\phi_b & \beta_b\sin\phi_b \\ -\dfrac{1}{\beta_b}\sin\phi_b & \cos\phi_b \end{pmatrix}$$

$$= \begin{pmatrix} \cos\phi_g\cos\phi_b - \dfrac{\beta_g}{\beta_b}\sin\phi_g\sin\phi_b & \beta_b\cos\phi_g\sin\phi_b + \beta_g\cos\phi_b\sin\phi_g \\ -\dfrac{1}{\beta_g}\cos\phi_b\sin\phi_g - \dfrac{1}{\beta_b}\cos\phi_g\sin\phi_b & -\dfrac{\beta_b}{\beta_g}\sin\phi_b\sin\phi_g + \cos\phi_g\cos\phi_b \end{pmatrix} , \tag{2.6}$$

where the equivalent betatron functions in the bunch and in the gap are, respectively,

$$\beta_b = \frac{\beta c}{\Omega_{eb}} \qquad \text{and} \qquad \beta_g = \frac{\beta c}{\Omega_{eg}} \ . \tag{2.7}$$

The condition for the electrons to escape is therefore

$$\frac{1}{2}|\mathrm{Tr}M| = \left|\cos\phi_g\cos\phi_b - \frac{1}{2}\left(\frac{\Omega_{eb}}{\Omega_{eg}} + \frac{\Omega_{eg}}{\Omega_{eb}}\right)\sin\phi_g\sin\phi_b\right| > 1 \ . \tag{2.8}$$

It is easy to demonstrate that Eq. (2.8) becomes Eq. (2.3) when $\eta \to 0$. For the Fermilab future booster, $\frac{1}{2}\mathrm{Tr}M$ is plotted in Fig. 1 as a function of the fractional proton leakage η into the gap. When the points are outside the ± 1 dashed lines, electrons can escape. It appears that when $\eta \gtrsim 0.030$, electrons will be trapped.

Figures 2, 3, and 4 show $\frac{1}{2}\mathrm{Tr}M$, respectively, for the ORNL SNS, LANL PSR, and BNL Booster. For the ORNL SNS, $\frac{1}{2}\mathrm{Tr}M$ oscillates rapidly with the fractional leakage. It appears that electrons will be trapped only if $\eta > 0.087$. For the LANL

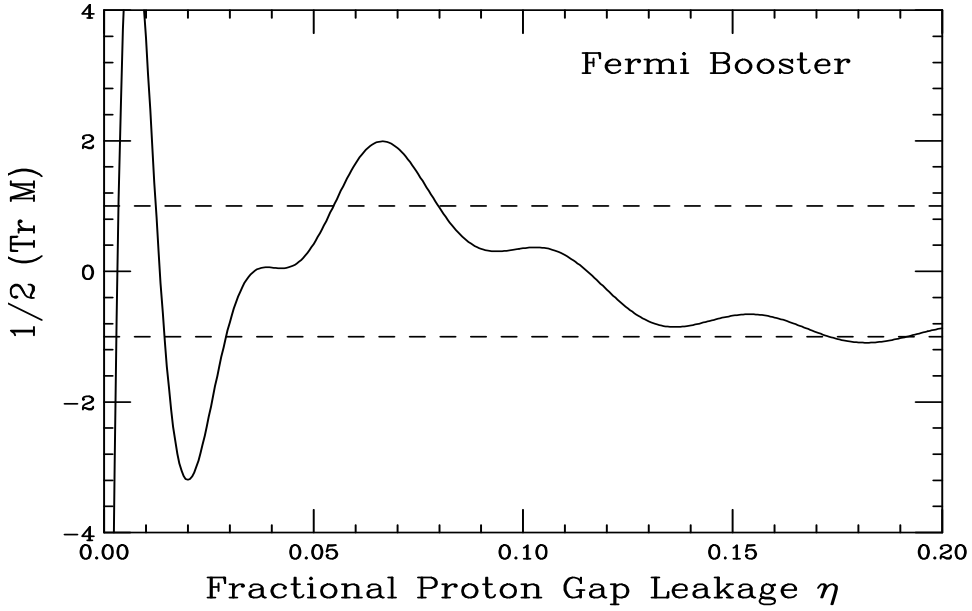

Figure 1: The Fermilab Future Booster: Electrons will be trapped if $\frac{1}{2}\mathrm{Tr}M$ falls between the ± 1 dashed lines.

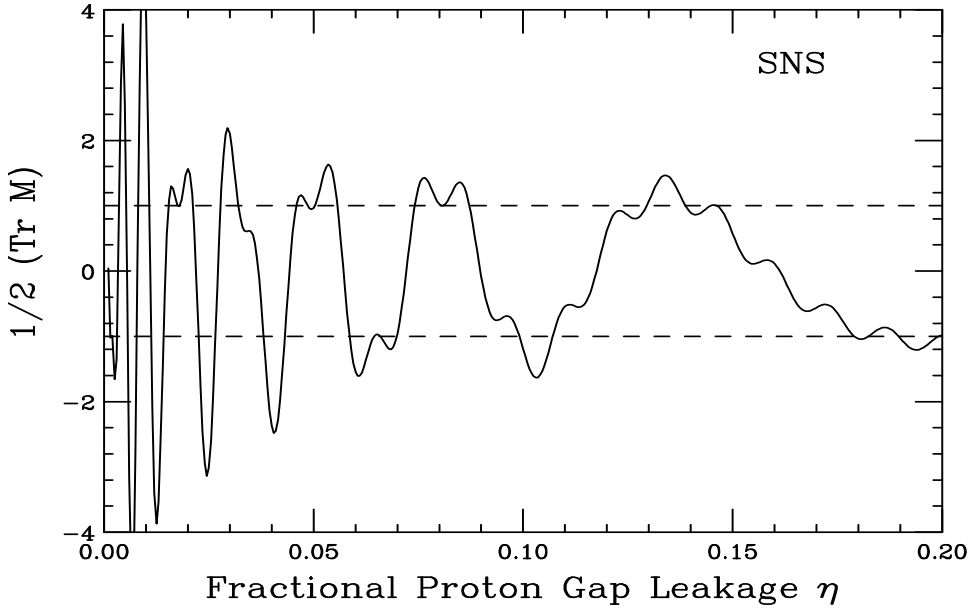

Figure 2: The ORNL SNS: Electrons will be trapped if $\frac{1}{2}\mathrm{Tr}M$ falls between the ± 1 dashed lines.

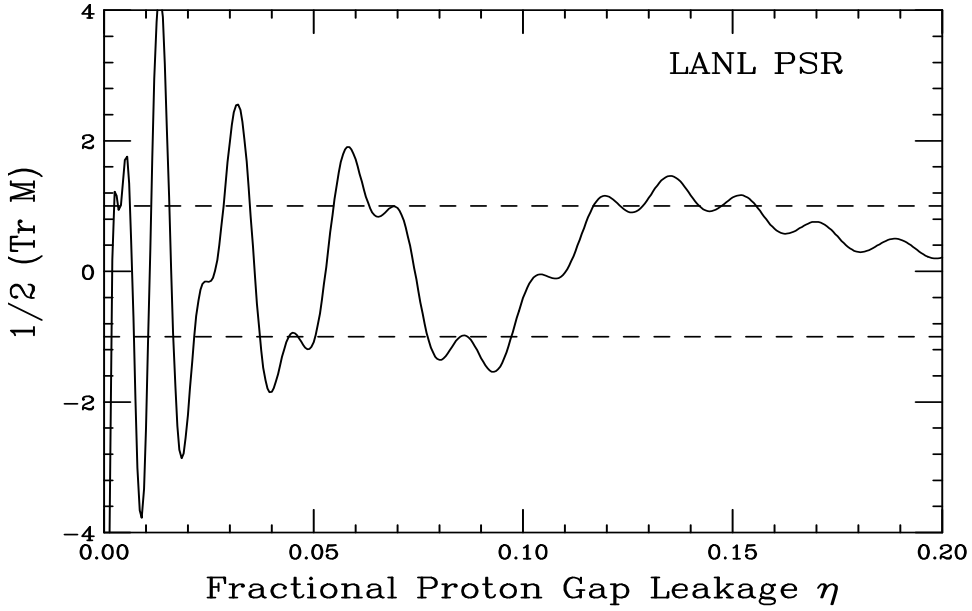

Figure 3: The LANL PSR: Electrons will be trapped if $\frac{1}{2}\mathrm{Tr}M$ falls between the ± 1 dashed lines.

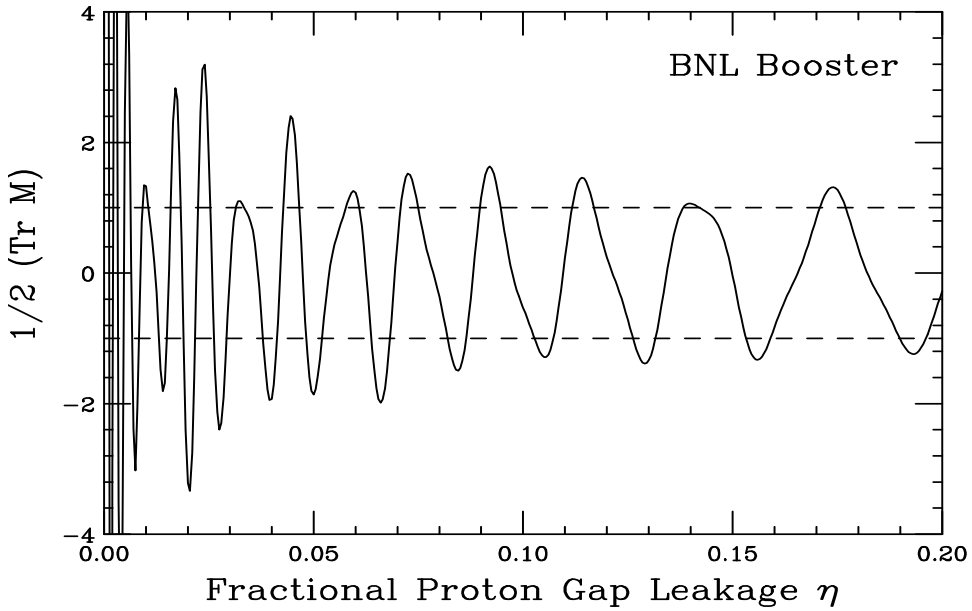

Figure 4: The BNL Booster: Electrons will be trapped if $\frac{1}{2}\mathrm{Tr}M$ falls between the ± 1 dashed lines.

PSR, electrons will probably be trapped if $\eta = 0.015$. For the BNL Booster, $\frac{1}{2}\mathrm{Tr}M$ oscillates very rapidly with η and electron will be trapped only if $\eta \gtrsim 0.05$.

III CENTROID-OSCILLATION INSTABILITY

Consider coupled oscillation of the proton beam and the electron 'beam' in the vertical direction. The displacements of a proton and electron from the central axis of the vacuum chamber are denoted, respectively, by y_p and y_e. Here, we assume both the proton and electron beams are coasting beams having the same transverse sizes and uniform distribution longitudinally and transversely. The coupled equations of motion are [7, 2, 3, 9]

$$\left(\frac{\partial}{\partial t} + \omega_0 \frac{\partial}{\partial \theta}\right)^2 y_p + Q_\beta^2 \omega_0^2 y_p = -Q_p^2 \omega_0^2 (y_p - \bar{y}_e) + Q_{ps}^2 (y_p - \bar{y}_p) \ , \tag{3.1}$$

$$\frac{d^2 y_e}{dt^2} = -Q_e^2 \omega_0^2 (y_e - \bar{y}_p) + Q_{es}^2 (y_p - \bar{y}_p) \ , \tag{3.2}$$

where $\bar{y}_p$ and $\bar{y}_e$ are the vertical displacements of the centroids of, respectively, the proton and electron beams from the axis of the vacuum chamber, ω_0 is the angular revolution frequency, θ is the azimuthal angle around the ring, Q_β is the betatron tune, and Q_p and Q_e are, respectively, the oscillation tune of the electrons inside the proton beam and the oscillation tune of the protons inside the electron beam. We have

$$\Omega_e^2 = (Q_e \omega_0)^2 = \frac{4 N_p r_e c^2}{a'(a+a')C} \ , \tag{3.3}$$

$$\Omega_p^2 = (Q_p \omega_0)^2 = \frac{4 N_p r_p c^2 \chi_e}{a'(a+a')\gamma C} \ , \tag{3.4}$$

where χ_e is the neutralization factor, or the ratio of the electron distribution to the proton distribution. In above, r_p is the classical proton radius, r_e the classical electron radius, and C the circumference of the accelerator ring. The negative signs on first terms on the right hand sides of Eqs. (3.1) and (3.2) indicate that the protons are focused by the electron beam and the electrons are focused by the proton beam. The factor γ in the denominator of Ω_p^2 comes about because the protons are circulating

around the ring while the electrons do not. Again, we are considering uniformly and cylindrical-symmetrically distributed proton and electron beams of radius a; or $a'(a+a') \to 2a^2$. Image effects in the walls of the vacuum chamber as well as nonlinear focusing forces are neglected.

The last term in the proton equation denotes the oscillations of the proton under the self-field of the proton beam. Here,

$$(Q_{ps}\omega_0)^2 = \frac{4N_p r_p c^2}{a'(a+a')\gamma^3 C} \tag{3.5}$$

is proportional to the linear space-charge tune shift of the proton beam. Similarly the last term in the electron equation, with

$$Q_{es}^2 = Q_e^2 \chi_e \tag{3.6}$$

denoting the space-charge tune shift of the electron beam, depicts the corresponding oscillations of the electron in the self-field of the electron beam.

Averaging over the proton displacements and electron displacements, we obtain the equations for the coupled motion of the proton-beam centroid $\bar{y}_p$ and the electron-beam centroid $\bar{y}_e$. Notice that the space-charge terms, Q_{ps}^2 and Q_{es}^2, drop out. If there is a coherent instability occurring at the angular frequency $\omega = Q\omega_0$, we can write

$$\bar{y}_p \sim e^{i(n\theta - \omega t)} \qquad \text{and} \qquad \bar{y}_e \sim e^{i(n\theta - \omega t)} \ , \tag{3.7}$$

where n is the longitudinal harmonic number. The coupled equations can be readily solved to give

$$(Q^2 - Q_e^2)[(n-Q)^2 - Q_\beta^2 - Q_p^2] - Q_e^2 Q_p^2 = 0 \ , \tag{3.8}$$

which is a quartic. For a solution when Q is near Q_e, we can expand Q around Q_e. When Q_p or the neutralization factor χ_e is large enough, the solution becomes complex and an instability occurs. The limiting Q_p is given by

$$Q_p \gtrsim \frac{|(n-Q_e)^2 - Q_\beta^2 - Q_p^2|}{2\sqrt{Q_e|n-Q_e|}} \ , \tag{3.9}$$

from which the limiting neutralization factor χ_e can be obtained. Once above threshold, the growth rate, given by

$$\frac{1}{\tau} = \frac{Q_p \omega_0}{2} \sqrt{\frac{Q_e}{|n-Q_e|}} \ , \tag{3.10}$$

is very fast. Notice that Q_p^2 on the right side of Eq. (3.9) in the numerator can be neglected because usually $Q_p^2 \ll Q_\beta$.

A proper employment of Eq. (3.9) is important, because it can give meaningless result. For example, in the situation:

$$[Q_e] = [Q_\beta] \qquad \text{or} \qquad [Q_e] + [Q_\beta] = 1 \ , \tag{3.11}$$

where $[Q_e]$ and $[Q_\beta]$ are, respectively, the residual betatron tune and the residual electron bounce tune, there will always exist a harmonic n which leads to instability for $Q_p \to 0$ or neutralization $\chi_e \to 0$. However, the growth rate will go to zero also. In reality, there is always a variation in the proton linear density or the electron bounce tune Q_e usually has a spread. Also the betatron tune can be suitably adjusted. For this reason, to estimate the threshold, we first compute Q_e from Eq. (3.3). Then the most offending harmonic n is determined as the integer closest to $Q_e + Q_\beta$. We next modify Q_e slightly so that

$$n - Q_e - Q_\beta = \frac{1}{2} \ . \tag{3.12}$$

Notice that one can also determine n as the integer closest to $|Q_e - Q_\beta|$. However, the threshold neutralization will in general be higher than that obtained by the first method if a difference less than $\frac{1}{2}$ is used on the right side of Eq. (3.12).

With this consideration, the results are listed in Table III. Here, the intensity of 4.42×10^{13} protons is used for the Brookhaven booster, where coasting beam experiments with possible e-p instabilities have been observed. We notice that the neutralization threshold is about $\chi_e = 0.52\%$ for the Fermilab future booster, 1.2% for the ORNL SNS, 0.9% for the LANL PSR, and 1.3% for the BNL booster. Once the thresholds are reached, the growth rates are very fast and the corresponding growth times are less than one turn for all the 4 machines.

There is another consideration of the stability of the two beam centroids, since the coherent oscillation can be stabilized by Landau damping. The equation of motion of the electron, Eq. (3.2), can be viewed as an undamped oscillator driven by $\bar{y}_p$, the centroid of the proton beam. Thus, spreads in the proton betatron tune Q_β and/or proton bounce tune Q_p alone will not be able to damp the electron oscillations. To damp the electron oscillation, there must be a spread in the electron bounce tune Q_e.

Table III: Coherent centroid-oscillation instability for proton-electron coasting beams.

	Fermilab Booster	Oak Ridge SNS	Los Alamos PSR	Brookhaven Booster
Total number of protons N_p	3.36×10^{13}	10.0×10^{13}	4.2×10^{13}	4.42×10^{13}
Betatron tune Q_β	10.60	5.82	2.14	4.80
Proton beam radius a (m)	0.0235	0.0380	0.0150	0.0150
$Q_p/\sqrt{\chi_e}$	2.155	1.2501	1.000	1.313
Most offending harmonic n	121	83	61	67
$Q_e = n - Q_\beta - \frac{1}{2}$	109.90	76.68	58.36	79.70
Limiting Q_p	0.1553	0.1379	0.0963	0.1229
Limiting neutralization χ_e	0.0052	0.0122	0.0093	0.0132
Growth rate in number of turns	0.651	0.663	0.703	0.668
Landau damping with $(\Delta Q_\beta - 2\Delta Q_{sc})/Q_\beta = 0.03$ and $\Delta Q_e/Q_e - \chi_e = 0.1$				
Limiting Q_p	0.5806	0.3188	0.1172	0.2629
Limiting neutralization χ_e	0.0726	0.0650	0.0137	0.0604
Growth rate in number of turns	0.171	0.279	0.587	0.311

The same applies to the equation of motion of the proton, Eq. (3.1), driven by the centroid of the electron beam. Therefore, to provide Landau damping to the coupled-centroid oscillation, there must exist large enough spreads in both the betatron tune ΔQ_β and the electron bounce tune ΔQ_e. Assuming semi-circular distributions for the betatron tune and the electron bounce tune with half maximum spreads ΔQ_β and ΔQ_e, the stability limit derived by Laslett, Sessler, and Möhl can be written as [8]

$$\left[\Delta Q_\beta^2 - \left(\frac{Q_{ps}^2}{Q_p'}\right)^2\right]^{1/2}\left[\Delta Q_e^2 - \left(\frac{Q_{es}^2}{Q_e'}\right)^2\right]^{1/2} \geq \frac{Q_p^2 Q_e^2}{Q_p' Q_e'}\ , \tag{3.13}$$

where we have denoted

$$Q_p'^{\,2} = Q_\beta^2 + Q_p^2 + Q_{ps}^2 \qquad \text{and} \qquad Q_e'^{\,2} = Q_e^2 + Q_{es}^2\ . \tag{3.14}$$

Notice that the space-charge self-force terms of Eqs. (3.1) and (3.2) do not drop out when averaged over the distributions. As an approximation, $Q_p' \sim Q_\beta$ implying

that $Q_{ps}^2/Q_p' \sim 2\Delta Q_{sc}$, where ΔQ_{sc} is the linear space-charge tune shift of the proton beam. Similarly, we can write $Q_{es}^2/Q_e' \sim Q_e\chi_e$, which is twice the linear space-charge tune shift of the electron beam. The stability condition then simplifies to

$$\left[\Delta Q_\beta^2 - 4\Delta Q_{sc}^2\right]^{1/2}\left[\Delta Q_e^2 - \chi_e^2 Q_e^2\right]^{1/2} \gtrsim \frac{Q_p^2 Q_e}{Q_\beta} \ . \tag{3.15}$$

Because of the square roots on the left side of Eq. (3.15), we also require for stability,

$$\Delta Q_\beta \geq 2Q_{sc} \qquad \text{and} \qquad \frac{\Delta Q_e}{Q_e} \geq \chi_e \ . \tag{3.16}$$

We do not know the spread in the electron bounce frequency because it cannot be measured. However, we may guess that the half maximum fractional spread of the electron bounce tune is $\Delta Q_e/Q_e - \chi_e \sim 0.1$, and the half maximum fractional spread of the betatron tune in excess of twice the space-charge tune shift is $(\Delta Q_\beta - 2\Delta Q_{sc})/Q_\beta \sim 0.03$. The limiting Q_p and neutralization factor χ_e can now be computed and are also listed in Table III. We note that for the Fermilab future booster, the threshold Q_p has been nearly quadrupled and the threshold neutralization is now 7.26%, an increase of almost 14 times. If the production of electrons can be under control, it may be possible that centroid-oscillation instability will not occur. For the ORNL SNS and the Brookhaven booster, the threshold neutralization factors have also been increased to 6.5% and 6.0%, respectively, although not as large as the Fermilab future booster. For the LANL PSR, however, the neutralization threshold χ_e remains at $\sim$ 1.4%, without much increase with Landau damping. Further increase in threshold requires larger spreads in Q_e and Q_β. In fact, it has been demonstrated that anti-damping can even happen unless there is a large enough overlap between ΔQ_β and ΔQ_e [7]. Notice that these stability limits of the neutralization factor can be sensitive to the distributions of the betatron tune and the electron bounce tune.

A stability condition has also been derived by Schnell and Zotter [7] assuming parabolic distributions for the betatron tune and the electron bounce tune, but without consideration of the space-charge self-forces. They obtain

$$\frac{\Delta Q_\beta}{Q_\beta}\frac{\Delta Q_e}{Q_e} \gtrsim \frac{9\pi^2}{64}\frac{Q_p^2}{Q_\beta^2} \ . \tag{3.17}$$

Notice that the Schnell-Zotter criterion is essentially the same as the Laslett-Sessler-Möhl criterion, if we interpret ΔQ_β of the former as the half tune spread of the betatron tune *in excess* of twice the space-charge tune spread of the proton beam, and ΔQ_e as the half tune spread of the electron bounce tune *in excess* of twice the space-charge tune spread of the electron beam. The factor $9\pi^2/64$ in Eq. (3.17) is probably a form factor of the parabolic distributions. Our discussion can be generalized when we notice that both Q_{ps}^2/Q_p' and Q_{es}^2/Q_e' in Eq. (3.13) come from, respectively, the $\bar{y}_e$ term in Eq. (3.1) and the $\bar{y}_p$ term in Eq. (3.2). Thus, Q_{ps}^2 and Q_{es}^2 can be extended to include the perturbations of oscillations coming from all types of impedances of the accelerator ring. In that case, the Schnell-Zotter stability criterion should be valid if we interpret ΔQ_β as the half tune spread of the betatron tune in excess of what is necessary to cope with the instabilities of the single proton beam, and ΔQ_e as the half tune spread of the electron bounce tune in excess of what is necessary to cope with the instabilities of the single electron beam.

IV PRODUCTION OF ELECTRONS

As seen in the previous section, the e-p coherent centroid-oscillation instability depends strongly on the neutralization factor, or the amount of electrons trapped inside the proton bunch.

One source of electron production is through collision of the protons with the residual gas in the vacuum chamber. At a vacuum pressure of 1×10^{-7} Torr, there is a residual gas density of $n_{\rm res} = 3.2 \times 10^9$ molecules/cm^3. The expected average ionization cross section is $\sigma_i = 1.2 \times 10^{-18}$ cm^2. If the residual gas is mostly bi-atomic molecules, each contributing two electrons, the rate of electron production is [5]

$$\frac{dN_e}{dt} = 2\beta c n_{\rm res} \sigma_i N(t) \ , \tag{4.1}$$

where $N(t)$ is the number of protons accumulated from injection at time t. If $t_{\rm inj}$ is the total injection time, $N(t) = N_p t/t_{\rm inj}$, where N_p is the total number of protons at the end of the injection. The neutralization due to ionization collision at the end of

injection is therefore

$$\chi_e = \frac{N_e}{N_p} = \beta c n_{\rm res} \sigma_i t_{\rm inj} \ . \tag{4.2}$$

The vacuum pressure for the ORNL SNS is designed to be 1×10^{-9} Torr and that for the LANL PSR is 2×10^{-8} Torr, while the other two rings are with vacuum pressure 1×10^{-7} Torr. The neutralization due to ionization collision turns out to be $\chi_e = 0.737\%$, 0.104%, 1.39%, and 2.33%, respectively, for the Fermilab future booster, ORNL SNS, LANL PSR, and BNL booster. The neutralization factors are large for PSR and the BNL booster because of their relatively low vacuum and long injection times of, respectively, ~ 2000 and 300 turns. The maximum neutralization of the ORNL SNS is small because of the very high vacuum. On the other hand, the Fermilab future booster is designed to have $\sim$ 27-turn injection and the maximum neutralization is therefore relatively lower.

Another source of electron production is through the multi-traversing of the stripping foil by the proton beam. For example, a proton in the LANL PSR can generate on the average two electrons because of the presence of the stripping foil.

A more important source of electron production is when an electron hitting the walls of the beam pipe releases secondary electrons. These secondary electrons can cause multipactoring and generate a large amount of electrons. Here, we would like to compute the energy of an electron hitting the beam pipe and estimate the efficiency of secondary emission [6].

An electron is oscillating with bounce frequency $\Omega_e/(2\pi)$ with amplitude increasing exponentially with an e-folding growth rate ω_I. Assume that the electron just grazes the wall of the beam pipe at time $t = 0$. Its amplitude is given by

$$y = be^{\omega_I t} \cos \Omega_e t \ , \tag{4.3}$$

where b is the beam pipe radius. It will hit the other side of the wall at time $t_1 = (\pi - \Delta)/\Omega_e$, where

$$-b = be^{\omega_I t_1} \cos \Omega_e t_1 = be^{(\pi-\Delta)\omega_I/\Omega_e} \cos(\pi - \Delta) \ , \tag{4.4}$$

which leads to

$$\Delta = \sqrt{\frac{2\pi\omega_I}{\Omega_e}} \left[1 + \mathcal{O}\left(\sqrt{\frac{\omega_I}{\Omega_e}} \right) \right] \ . \tag{4.5}$$

The velocity of the electron hitting the other side of the wall can be obtained by differentiating Eq. (4.3) and is given by

$$\dot{y} = \sqrt{2\pi\omega_I\Omega_e}\left[1 + \mathcal{O}\left(\sqrt{\frac{\omega_I}{\Omega_e}}\right)\right] \ . \tag{4.6}$$

The kinetic energy is therefore

$$E_{\rm kin} = \pi m_e \omega_I \Omega_e b^2 \ , \tag{4.7}$$

where m_e is the electron mass.

For single-electron motion, we can identify the growth rate $\omega_I = \mu\beta c/\lambda_{\rm rf}$, where μ is given by Eq. (2.4). The velocities and kinetic energies of the electrons hitting the wall on the other side of the beam pipe are listed in Table IV. We see that when hitting the beam pipe wall, the electrons possess kinetic energies of 34.9, 198.6, 775.4, and 139.5 eV, respectively, for the 4 rings. For the BNL booster, the bunched mode intensity has been used. It is a known fact that an electron in excess of 100 eV hitting a metallic wall will result in a secondary emission coefficient greater than unity. This implies that multipactoring will occur except for the Fermilab future booster. This consideration is for the motion of a single electron and is independent of the amount of electrons present in the ring. In the design of the ORNL SNS, the beam pipe will be made of stainless steel with a titanium coating, which will reduce the secondary emission efficiency and thus prevent multipactoring to occur. An experiment was performed at the LANL PSR by coating part of the walls of the vacuum chamber with TiN. The electron flux was found to have been suppressed about 1000 times [10].

We can also identify ω_I with the growth rate τ^{-1} of the coherent centroid oscillation in Eq. (3.10). The kinetic energy for an electron hitting the other side of the beam pipe wall becomes

$$E_{\rm kin} = \frac{\pi m_e Q_p Q_e^{3/2} \omega_0^2 b^2}{2\sqrt{|n - Q_e|}} \ . \tag{4.8}$$

Notice that the kinetic energy of the electron hitting the pipe wall is now proportional to Q_p and therefore $\sqrt{\chi_e}$. These are listed in Table IV at the threshold neutralization. Notice that the kinetic energies of the electrons hitting the beam pipe walls at the onset of coupled-centroid instability are less than 100 eV for the Fermilab future booster,

Table IV: Kinetic energy of electron hitting the wall of the beam pipe.

	Fermilab Booster	Oak Ridge SNS	Los Alamos PSR	Brookhaven Booster
Total number of protons N_p	3.36×10^{13}	10.0×10^{13}	4.2×10^{13}	2.4×10^{13}
Beam pipe radius b (m)	0.0635	0.0500	0.0500	0.0600
Single-electron consideration				
Electron escaping rate ω_I (MHz)	1.90	6.24	13.9	4.69
Ω_e (MHz)	255.1	713.3	1253.9	462.6
Velocity hitting wall $\dot{y}/c$	0.0117	0.0279	0.0551	0.0234
Kinetic energy hitting wall (eV)	34.9	198.6	775.4	139.5
Coherent-centroid-oscillation consideration				
Threshold neutralization χ_e	0.0052	0.0122	0.0093	0.0113
Growth rate ω_I (MHz)	0.461	1.793	3.976	1.258
Ω_e (MHz)	207.5	572.7	1025.2	325.7
Velocity hitting wall $\dot{y}/c$	0.0052	0.0134	0.0267	0.0102
Kinetic energy hitting wall (eV)	6.90	45.9	182.0	26.3

the ORNL SNS, and the BNL booster in the bunched mode. Thus multipactoring will occur only if the neutralization factor is much larger than $\sim 1\%$. On the other hand, the electron kinetic energy is 182 eV for the PSR. Thus multipactoring will occur before the onset of coherent centroid instability.

V DISCUSSIONS AND CONCLUSION

(1) In the above single-electron analysis, it appears that electrons will be cleared in the bunch gap within one rf wavelength for all the 4 proton rings under consideration. However, if more than $\eta = 3.0\%$ of the protons are spilled into the bunch gap, electrons will be trapped inside the proton beam in the Fermilab future booster and will be unable to escape. This is better than the LANL PSR, which will trap electrons if only $\eta = 0.2\%$ of the protons are spilled into the gap. However, the ORNL SNS and the BNL booster are relatively more stable, because they will only trap electrons if

more than, respectively, 8.7% and 5.0% of protons spilled into the gaps.

(2) For coherent centroid oscillation to become unstable, neutralization factors of $\chi_e \sim 0.52\%$, 1.2%, 0.9%, and 1.1% are required, respectively, for the 4 machines. However, spreads in the betatron frequencies and the electron bounce frequencies can provide Landau damping.

(3) Although the Fermilab future booster may have a low vacuum of $\sim 1 \times 10^{-7}$ Torr, due to its short injection time of 27 turns, the amount of electrons per proton produced by collision of the protons with the residual gas will be small, $\chi_e = 0.74\%$. On the other hand, $\chi_e \sim 7.0\%$ of electrons will be produced in the LANL PSR, which accumulates protons in ~ 2000 turns. The electron production for the ORNL SNS via proton-ion collision is less than 1%, which is the result of a high vacuum of 1×10^{-9} Torr in the vacuum chamber.

(4) Multipactoring as a result of secondary emission will not occur in the Fermilab future booster, but will be possible for all the other rings when single electron escapes from the trapping proton beam and hits the metallic beam pipe. For the LANL PSR, multipactoring will occur before the onset of coherent centroid instability. However, for the other 3 rings, multipactoring will not occur as soon as centroid oscillations become unstable.

(5) There is a similar proton ring called ISIS at the Rutherford Appleton Laboratory. At the injection energy of 70.4 MeV, about 2.5×10^{13} protons are stored as a continuous coasting beam, which is then captured adiabatically into 2 rf buckets. The protons are ramped to 0.8 GeV when they are extracted. No e-p instabilities have ever been observed at ISIS either running in the bunched mode or the coasting-beam mode. This has always been a puzzle. However, when we compare ISIS with the LANL PSR, we do find some important differences. First, ISIS has a repetition rate of 50 Hz. The injection is fast, about 200 turns. On the other hand, it usually takes about 200 turns for the e-p instability of the PSR to develop to a point when it can be monitored. Second, ISIS has a much larger vacuum chamber, 7 cm in radius. Also the ISIS vacuum chamber is made of ceramic to limit eddy current because of the high repetition rate of 50 Hz. However, a wire cage is installed inside the ceramic

beam pipe to carry the longitudinal return current. The wire cage does not allow transverse image current to flow, thus alleviating in some way the transverse instability. Also the cage wires have much less surface area than the walls of an ordinary metallic beam pipe. As a result, secondary emission will be reduced. The secondary emitted electrons will come out in all directions from the cage wires. The probability for them to hit another cage wire will be small, thus preventing multipactoring to occur. These may be the reasons why e-p instabilities have never been observed at ISIS.

(6) Because of the short injection time of the Fermilab future booster, coupled-centroid e-p instabilities may not have enough time to develop fully during injection. Since multipactoring will not occur, the neutralization factor will remain small. However, all these can be changed if the total intensity of the ring is upgraded to 1×10^{14} protons in the future. In the single-electron consideration, an electron hitting the walls of the beam pipe will have a kinetic energy well over 150 eV, implying that multipactoring will be possible, and when the neutralization factor is large enough, e-p instabilities will still occur. For this reason, method must of devised to get rid of the electrons produced during the multi-traversing of the stripping foil by the proton beam. At the same time, the vacuum pressure should be further reduced to preferably 1×10^{-9} Torr as in the ORNL SNS. If multipactoring occurs and the neutralization factor is large enough, e-p instabilities can also occur during the ramping stage of the booster, which we have not discussed here.

The author wishes to thank Dr. M. Blaskiewicz for very useful discussions and his careful reading of the manuscript.

References

[1] Fermilab Report, *The Feasibility of a Neutrino Source Based on a Muon Storage Ring*, ed. N. Holtkamp and D. Finley, 2000, web address: http://www.fnal.gov/projects/muon_collider/nu-factory/draft_report_march31st; Weiren Chou, *Proton Driver Study at Fermilab*, Fermilab Report Fernmilab-Conf-99/277, 1999.

[2] D. Neuffer, E. Colton, D. Fitzgerald, T. Hardek, R. Hutson, R. Macek, M. Plum, H. Thiessen, and T.-S.Wang, Nucl. Instr. Meth. **A321**, 1 (1992).

[3] M. Blaskiewicz, *The Fast Loss Electron Proton Instability*, Proceedings of the Workshop on Instabilities of High Intensity Hadron Beams in Rings, ed. T. Roser and S.Y. Zhang, Upton, N.Y., 1999, p. 321.

[4] In the reference below, aluminum pipe with titanium coating is mentioned: http://www.ornl.gov/∼nsns/CDRDocuments/CDRSections/CDRSections.html. In the more recent design, however, stainless steel beam pipe with TiN coating is used.

[5] A. Ruggiero and M. Blaskiewicz, *e-p Instabilities in the NSNS Accumulator Ring*, Proceedings of the 1999 Particle Accelerator Conference, New York, 1999, p.1581.

[6] M. Blaskiewicz, *Instabilities in the SNS*, Proceedings of the 1999 Particle Accelerator Conference, New York, 1999, p.1611.

[7] W. Schnell and B. Zotter, CERN Report ISR-GS-RF/76-26 (1976).

[8] L.J. Laslett, A.M. Sessler and D. Möhl, Nnucl. Inst. Meth. **121** 517 (1974).

[9] Tai-Sen F. Wang, *A Theoretical Study of Electron-Proton Instability I and II*, LANL Report PSR-96-004 and PSR-96-004 (1996).

[10] R. Macek, talk given at the 8th Advanced Beam Dynamics Mini-Workshop on Two-Stream Instabilities in Particle Accelerators and Storage Rings, Santa Fe, New Mexico, February 16-18, 2000